Case Studies in Construction Materials 17 (2022) e01431

Contents lists available at ScienceDirect

Case Studies in Construction Materials

journal homepage: www.elsevier.com/locate/cscm

Material enhancements of newly developed stiff type polyurea for retrofitting of concrete structures

Tae-Hee Lee[a,1], Jun-Hee Park[a,2], Dal-Hun Yang[b,3], Jang-Ho Jay Kim[a,*,4], Norhazilan Bin Md. Noor[c,5]

[a] *School of Civil and Environmental Engineering, Yonsei University, 50 Yonsei-Ro, Seodaemun-Gu, Seoul 03722, the Republic of Korea*
[b] *Central Research Institute, Korea Hydro & Nuclear Power Co., 70 Yuseong-daero 1312 gil, Yuseong-gu, Daejeon, the Republic of Korea*
[c] *Department of Structure and Materials, Universiti Teknologi Malaysia, Sultan Ibrahim Chancellery Building, Jalan Iman, 81310 Skudai, Johor, Malaysia*

A R T I C L E I N F O

Keywords:
Seismic loadings
Retrofitting materials
Strengthening materials
Stiff-type polyurea
Material properties

A B S T R A C T

Recently, polyurea (PU) has been receiving great interest from the construction industry as a structural retrofitting and strengthening material due to its simple application of spraying on the structural member surface without creating an epoxy bonding interface. In this study, based on knowledge gained from developing flexible-type PU (FTPU) in preceding studies, stiff-type PU (STPU) is developed by varying the prepolymer/hardener ratio of FTPU. A mechanical property evaluation of STPU is performed through tensile strength, percent elongation, pull-off, and Shore hardness tests. Furthermore, a durability property evaluation of STPU is performed through acid environmental and ultraviolet (UV) exposure tests. In addition, concrete carbonation exposure and freeze–thaw tests are performed for STPU. The experimental results show that STPU has a higher tensile strength and lower elongation percentage than FTPU with excellent mechanical and durability properties. Using the optimal mix proportion of STPU, the surfaces of concrete specimens sprayed with STPU are tested under uniaxial compression loading. The uniaxial test results show that the strengthened concrete specimens have maximum load ratios 1.14–1.20 times those of the non-strengthened concrete specimens. Based on the test results, STPU can be used as a retrofitting and strengthening material for concrete members to resist seismic and extreme loading (e.g., impact, blast).

Abbreviation: PU, polyuria; FTPU, fexible-type polyuria; STPU, stiff-type polyuria; UV, ultraviolet; HDI, hexane diisocyanate; IPDI, isophorone diisocyanate; H12MDI, methylenebis(cyclohexyl diisocyanate); TDI, toluene diisocyanate; NDI, naphthalene diisocyanate; MDI, methylene diphenyl diisocyanate; TODI, bitoluene diisocyanate; BD, butanediol; ED, ethylene diamine; MBOCA, methylenebis 2-chloroaniline; EG, ethylene glycol; HD, hexanediol; C-RC, circular reinforced concrete column; C-STPU, circular STPU applied reinforced concrete column; S-RC, square reinforced concrete column; S-STPU, square STPU applied reinforced concrete column.

* Corresponding author.
E-mail address: jjhkim@yonsei.ac.kr (J.-H.J. Kim).
[1] ORCID number: 0000-0003-1457-4681.
[2] ORCID number: 0000-0002-0279-0937.
[3] ORCID number: 0000-0002-3996-7126.
[4] ORCID number: 0000-0002-5138-8282.
[5] ORCID number: 0000-0002-1374-0919.

https://doi.org/10.1016/j.cscm.2022.e01431
Received 26 June 2022; Received in revised form 13 August 2022; Accepted 23 August 2022
Available online 26 August 2022
2214-5095/

1. Introduction

Recently, 21, 7, 5, 2, and 1 cases of strong earthquakes exceeding 6.0 on the Richter scale were reported on Japanese seashores, on Taiwanese seashores, in inland Nepal, in inland China, and in inland Russia, respectively. In addition, earthquakes have caused serious human casualties and damage to critical structures and infrastructures in recent years, resulting in enormous economic losses and property damage [1]. In Korea, the number of earthquakes has increased over the past few years. For example, 93 earthquakes exceeding 2.0 on the Richter scale occurred in 2013, twice as many as the annual mean number of earthquakes (44.5) that occurred in Korea from 1999 to 2012 [2]. Furthermore, earthquakes exceeding 5.1 and 5.0 in magnitude on the Richter scale occurred on the west-central and southeastern seashore of the Korean Peninsula, respectively [1].

Although seismic design requirements were enacted by law on July 1, 1988, based on studies on earthquake-proof construction and disaster prevention in buildings in Korea, structures built before July 1988 are vulnerable to earthquakes. Various construction

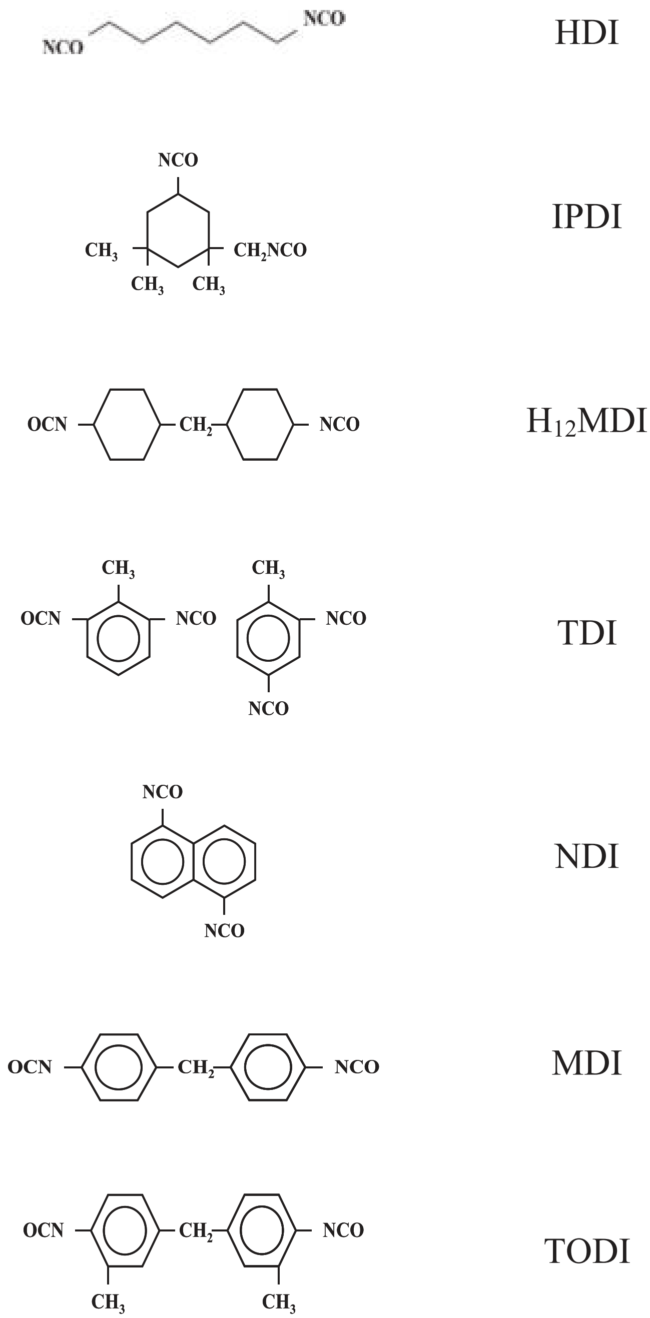

Fig. 1. Molecular formulae of diisocyanates.

techniques have been developed such as member cross-sectional enhancement, concrete material enhancement, steel plate and fiber-reinforced polymer (FRP) sheet surface wrapping for circular cross-sectional columns, and reinforcement addition [3–16]. The ultimate goal of seismic retrofitting and strengthening of structural members is to improve the load-carrying capacity, ductility, and shear strength such that the structural members would survive seismic loading from an earthquake. In particular, the method of attaching FRP sheets to surfaces has numerous advantages, including construction simplicity and relatively low cost. However, the method has disadvantages with respect to long-term service life due to deterioration of the bonding adhesives used to attach FRP to surfaces and deterioration of the FRP sheets themselves from exposure to outdoor weather conditions, which make the retrofitting work futile. Therefore, solving these problems necessitates the development of new materials and techniques that can induce monolithic behavior and eliminate the interface between the structure and retrofitting material while delivering material performance equivalent to that of FRP.

The construction material polyurea (PU) has been suggested as an alternative retrofitting material to FRP. PU is a polymer-based, high-ductility material made using highly polymerized compounds. PU is normally a nonstructural material that can be used in many applications. PU has been widely used as a waterproofing material because of its excellent moisture protection and tensile strength. However, the chemical composition of PU must be extensively adjusted for it to be used as a structural retrofitting material. A previous study on the development of flexible-type PU (FTPU) showed that the strengthening performance of PU can be improved by adjusting its chemical properties; however, an evaluation of the strengthening performance of FTPU showed that further improvements are needed for it to be safely used for structural retrofitting and strengthening applications [17]. A critical property of FTPU that hinders its use in retrofitting structural applications is its stiffness. After FTPU is sprayed onto the target retrofit member to a certain thickness, the hardened FTPU must exhibit sufficient stiffness to improve the retrofitted member's load-carrying and energy-absorption capacities. One approach to solving this issue is to convert FTPU to stiff-type PU (STPU) by changing the composition of FTPU.

In the present work, numerous trial-and-error variations of the mix proportion were investigated to develop STPU with sufficient stiffness and strength to be tested for tensile strength, percent elongation, pull-off, and Shore hardness properties. Moreover, evaluations of the durability of STPU under exposure to acid, ultraviolet (UV) light, and carbonation conditions as well as freeze–thaw studies on concrete specimens covered with STPU were conducted.

The test results showed that using STPU for structural retrofitting applications is feasible [18–20]. STPU exhibited improvements in tensile strength, elastic modulus, and percent elongation compared with FTPU. Using the optimal mix proportion of STPU obtained from the material development phase, we prepared cylindrical and rectangular concrete specimens whose surface was sprayed with STPU and then tested them under uniaxial compression loading. The study results are discussed in detail in the paper.

2. STPU

2.1. Basic components of PU

PU is produced by mixing a prepolymer and a hardener. The prepolymer is prepared by mixing isocyanate and a diol (diamine),

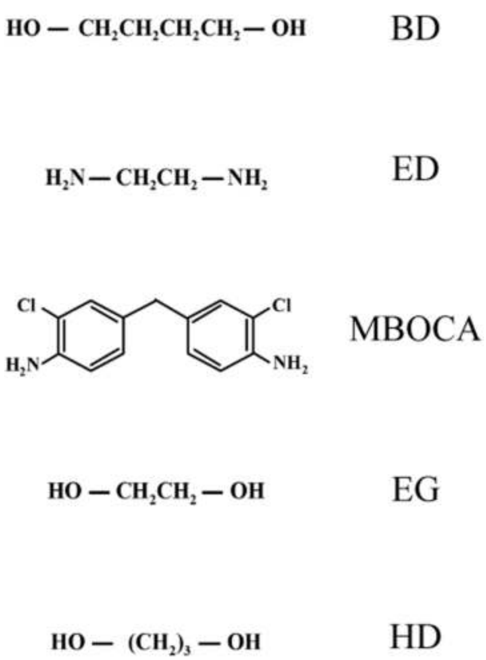

Fig. 2. Molecular formulae of chain extenders.

resulting in a compound known as a diisocyanate. Diisocyanates are classified into aliphatic, aromatic, and cycloaliphatic diisocyanates, all of which can be used as prepolymers. Aliphatic diisocyanates include hexane diisocyanate (HDI), isophorone diisocyanate (IPDI), and methylenebis(cyclohexyl diisocyanate) (H12MDI). Aromatic diisocyanates include toluene diisocyanate (TDI), naphthalene diisocyanate (NDI), methylene diphenyl diisocyanate (MDI), and bitoluene diisocyanate (TODI). Cycloaliphatic diisocyanates are composed of an isocyanate combined with methylene and cyclohexane. The molecular formulae of diisocyanates used for PU synthesis in the present work are shown in Fig. 1 [21].

For the hardener, a diamine chain extender of PU, butanediol (BD), ethylene diamine (ED), methylenebis 2-chloroaniline (MBOCA), ethylene glycol (EG), or hexanediol (HD) is commonly used. The molecular formulae of the chain extenders used for PU synthesis in the present work are shown in Fig. 2 [21]. The chain extender used in a PU hardener is a monomer or oligomer, which increases the molecular weight of the PU; molecular weight plays an important role in increasing the bond strength of PU as well as in improving its density and mechanical properties. The diamine chain extender used in this study reacts with isocyanate rapidly and violently to form a urea group as well as a biuret bond between chains (a "biuret bond" refers to a substance produced via the reaction between isocyanate and hydrogen, which is present on the nitrogen atoms in urea groups and exhibits high reactivity). Because the highly reactive polymers are formed in a short time, the overall process can be reduced to a single step, which is advantageous.

2.2. Development of STPU

To develop STPU with a high tensile strength and low percent elongation, three cases of prepolymer types are selected for STPU, as shown in Table 1. For each type of prepolymer, NCO percentages of 13 %, 15.5 %, and 18 % are added to STPU to test its tensile strength, percent elongation, and Shore hardness properties, as shown in Table 1. Based on the evaluated properties, the optimal prepolymer type and NCO amount are selected for the mixing of STPU.

The composition ratio between the prepolymer and hardener was modified to develop the three types of STPU as follows:

1) For the prepolymer synthesis of Case 1, P,P′- 4,4′-methylene diphenyl diisocyanate (MDI) 53 %, alpha-(2-aminomethylethyl)-omega-(2-aminomethylethoxy)-poly(oxy(methyl-1,2-ethanediyl)) 27 %, polyoxypropylene glycol 19 %, and propylene carbonate 1 % were used. For the hardener synthesis of Case 1, alpha-(2-aminomethylethyl)-omega-(2-aminomethylethoxy)-poly(oxy(methyl-1,2-ethanediyl)) 72.1 %, 3,5 diethyltoluene-2,4/2,6-diamine 25.9 %, 4,4′-methylene bis[N-(1-methylpropyl)benzenamine 1.6 %, and UV sorbent under 0.5 % were used.

2) For the prepolymer synthesis of Case 2, P,P′- methylene bisphenyl isocyanate (MDI) 42 %, methylenebis(4,1-phenylene) diisocyanate (MDI) 10 %, alpha-(2-aminomethylethyl)-omega-(2-aminomethylethoxy)-poly(oxy(methyl-1,2-ethanediyl)) 39.5 %, and propylene carbonate 8.5 % were used. For the hardener synthesis of Case 2, alpha-(2-aminomethylethyl)-omega-(2-aminomethylethoxy)-poly(oxy(methyl-1,2-ethanediyl)) 70.1 %, poly[oxy(methyl-1,2-ethanediyl)],.alpha.,.alpha.',.alpha.'' – 1,2,3-propanetriyltris[.omega.-(2-aminom,ethylethoxy) 9.0 %, 3,5 diethyltoluene-2,4/2,6-diamine 15.4 %, 4,4′-methylene bis[N-(1-methylpropyl)benzenamine 5.0 %, and UV sorbent under 0.5 % were used.

3) For the prepolymer synthesis of Case 3, methylenebis(4,1-phenylene)diisocyanate (MDI) 64.5 %, alpha-(2-aminomethylethyl)-omega-(2-aminomethylethoxy)-poly(oxy(methyl-1,2-ethanediyl)) 27.5 %, polyoxypropylene glycol 5 %, and propylene carbonate 1 % were used. For the hardener synthesis of Case 3, alpha-(2-Aminomethylethyl)-omega-(2-aminomethylethoxy)-poly(oxy(methyl-1,2-ethanediyl)) 24.6 %, 3,5 diethyltoluene-2,4/2,6-diamine 11.9 %, 4,4′-methylene bis[N-(1-methylpropyl)benzenamine 32.6 %, 4,4′-methylene bis (2-chloroaniline) 29.4 %, and UV sorbent under 1.5 % were used.

As shown in Cases 1–3, STPU was polymerized with different ratios of the prepolymer and hardener at temperatures ranging from

Table 1
Composition of STPU.

Material	Component		Case 1	Case 2	Case 3
			Weight		
Prepolymer	MODIFIED MDI	(P,P′- METHYLENE BISPHENYL ISOCYANATE)	–	42 %	–
	Monomeric MDI	(4,4′-Methylene diphenyl diisocyanate)	53 %	–	–
	Polymeric MDI	Methylenebis(4,1-phenylene)diisocyanate	–	10 %	64.50 %
	Polyol	Alpha-(2-aminomethylethyl)-omega-(2-aminomethylethoxy)-poly(oxy(methyl-1,2-ethanediyl))	27 %	39.50 %	27.50 %
		Polyoxypropylene glycol	19 %	–	5 %
	Additive	Propylene carbonate	1 %	8.50 %	3 %
Hardener	JEFFAMINE	Alpha-(2-aminomethylethyl)-omega-(2-aminomethylethoxy)-poly(oxy(methyl-1,2-ethanediyl))	72.1 %	70.1 %	24.6 %
		Poly[oxy(methyl-1,2-ethanediyl)],.alpha.,.alpha.',.alpha.'' – 1,2,3-propanetriyltris[.omega.-(2-aminom,ethylethoxy)	–	9.0 %	–
	FUNCTIONAL AMINE	3,5 Diethyltoluene-2,4/2,6-diamine	25.9 %	15.4 %	11.9 %
		4,4′-Methylene bis[N-(1-methylpropyl)benzenamine	1.6 %	5.0 %	32.6 %
		4,4′-Methylenebis(2-chloroaniline)	–	0.0 %	29.4 %
	UV additive (UV sorbent)	ZIKASORB-BS	0.5 %	0.5 %	1.5 %

30 to 90 ℃ (e.g., optimum at 75 ℃).

3. STPU mechanical property tests

Mechanical property tests of tensile strength, percent elongation, pull-off, and Shore hardness were conducted on the three types of STPU specimens.

3.1. Tensile strength and percent elongation test descriptions and discussion of results

Tensile strength and percent elongation tests were conducted in accordance with KS M 6518 [22]. The purpose of the tests was to measure the maximum stress (tensile strength) and the percent elongation when ultimate fracture failure occurred in the STPU specimens. The test specimens were cut from STPU pallets into a type 3 dumbbell shape, as specified in KS M 6518 [22]. Its horizontal width, length, and thickness were 5 mm, 20 mm, and 3 mm, respectively, and the gradation distance was 20 mm, as shown in Fig. 3(a). The cutter used is shown in Fig. 3(b). As shown in Fig. 3(c), tensile strength and percent elongation were measured by fixing a specimen at both ends, where clamps were used to prevent the specimen from twisting and releasing during the test. The tensile tester was set to have a maximum load of 15–85 % of the design maximum load. A tensile load was applied as a displacement control load with a loading rate of 8.33 mm/s. The loading rate of 8.33 m/s is selected based on trial tests such that the unstable or end section premature failure does not occur during the test. When the maximum load was reached, the specimen was cut, and the cross-sectional area was measured for the calculation of the strength using Eq. 1.

$$T_B = F_B/A \tag{1}$$

where T_B is the tensile strength (MPa), F_B is the maximum load (N), and A is the cross-sectional area of the specimen (mm^2). The mean strength of three specimens was taken as the tensile strength.

Table 2 and Fig. 4(a) show the results of the tensile strength tests. The tensile strength results showed the trend of Case 3 > Case 2 > Case 1, with Case 3 having the highest strength. In Case 3, NCO (%) mix ratios of 13 %, 15.5 %, and 18 % gave tensile strength values of 21, 25, and 28 MPa, respectively, which showed that the greatest strength was achieved with the highest NCO mix ratio of 18%. In the other two cases, the same trend was observed. The test results showed that the strength increases with the amount of isocyanate, as shown in Table 1.

To obtain the percent elongation, we measured the length between gradations at the time of ultimate fracture and then calculated the percent elongation E_B using Eq. 2.

$$E_B = \frac{L_l - L_0}{L_0} \times 100 \tag{2}$$

where L_0 is the initial length (mm) and L_l is the length at rupture (mm). The mean percent elongation of three specimens was taken as the percent elongation.

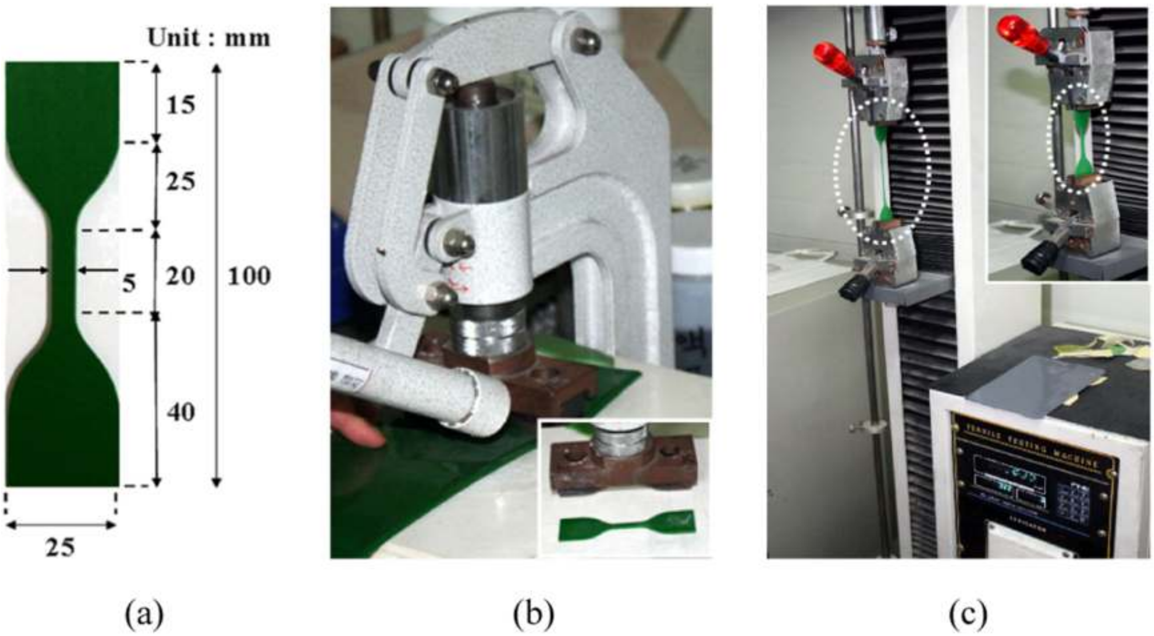

Fig. 3. (a) Type 3 dumbbell specimen details; (b) specimen cutter; (c) tensile strength test setup.

Table 2
Tensile strength and percent elongation test results.

	NCO [%]	Tensile strength [MPa]	Percent elongation [%]
Case 1	13	15	300
	15.5	18	250
	18	21	170
Case 2	13	18	150
	15.5	22	120
	18	25	100
Case 3	13	21	320
	15.5	25	280
	18	28	250

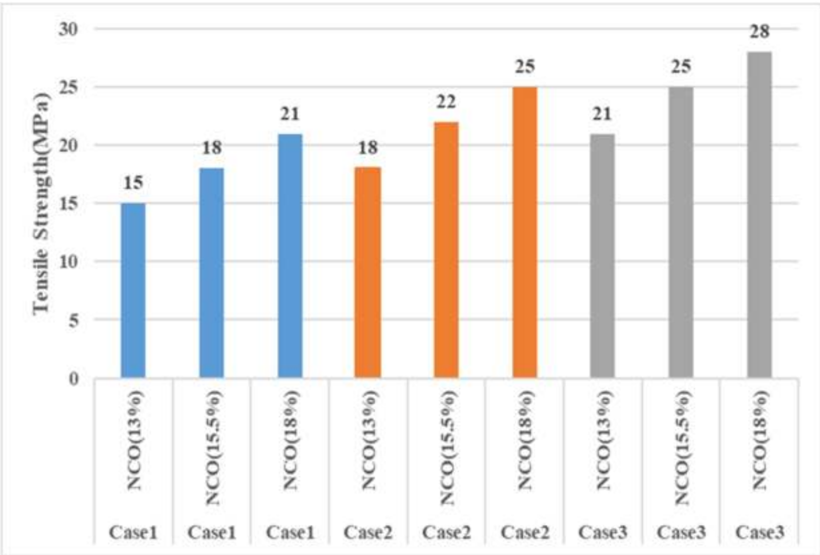

(a)

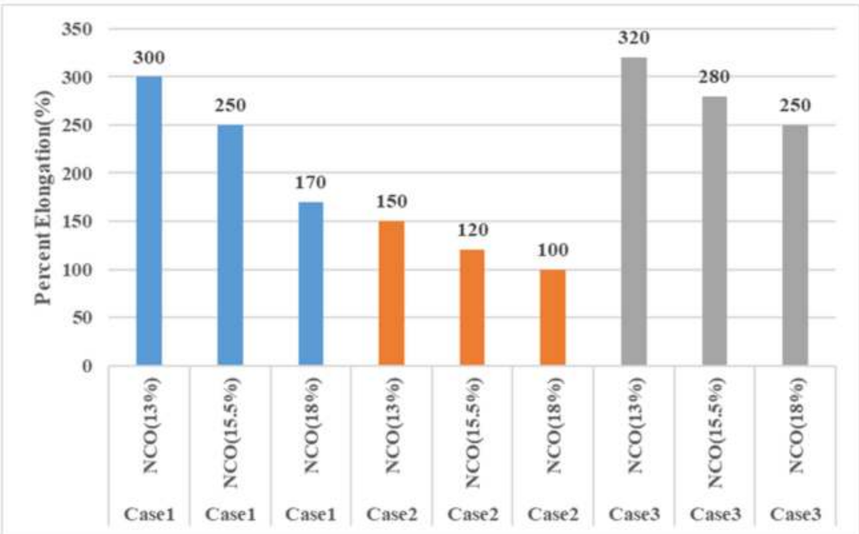

(b)

Fig. 4. (a) Tensile strength test results; (b) percent elongation test results.

Table 2 and Fig. 4(b) show the percent elongation results. The percent elongation of Case 2 was lowest with brittle failure behavior, followed by Case 1 and then 3. In all cases, as the NCO mix ratio increased, the percent elongation decreased. From the perspective of structural retrofitting and strengthening, the structural performance improvement effect diminishes since the applied PU prematurely fails prior to achieving the significant repairing effect. Therefore, it is important to develop STPU that has both high tensile strength and percent elongation properties.

3.2. Pull-off test description and discussion of results

One of the main methods used to evaluate the bonding property of strengthening materials is the pull-off test. Because the most critical problem in the FRP surface-bonding method is the bonding performance between a retrofitting material and the concrete member surface, we evaluated the bonding property of the STPU. Pull-off tests were conducted in accordance with KS F 4922 [23]. For the base plate in the test, a concrete slab with dimensions 300 mm × 300 mm × 60 mm was used. STPU was then applied to the top surface of the concrete slab and allowed to dry. As shown in Fig. 5(a), a tension screw dolly was attached to the STPU-applied specimen using a two-part epoxy adhesive; the attachment area was 40 mm × 40 mm. The 40 mm × 40 mm STPU–concrete section was then cut out using a grinder cutter [23]. A tension jig was screwed to the dolly to be connected to the tester, as shown in Fig. 5(b), which depicts the front view of the pull-off test setup. Three tests were performed for each case to calculate the mean bond strength. The displacement-controlled tensile load with a rate of 0.033 mm/s was applied. Eq. 3 was used to calculate the maximum strength.

$$T_f = F_n / A \tag{3}$$

where T_f is the bond strength (MPa), F_n is the maximum load (N), and A is the area of the specimen (mm^2).

According to the test results, the bond strengths in all cases were 1.5–2.5 MPa. In all cases, the PU bond strength requirement of 1.5 MPa of the Korean standard was satisfied [23].

3.3. Shore hardness and drying time test descriptions and discussion of results

Measuring hardness is one of the simplest methods to determine material rigidity, which is directly related to elastic modulus, heat

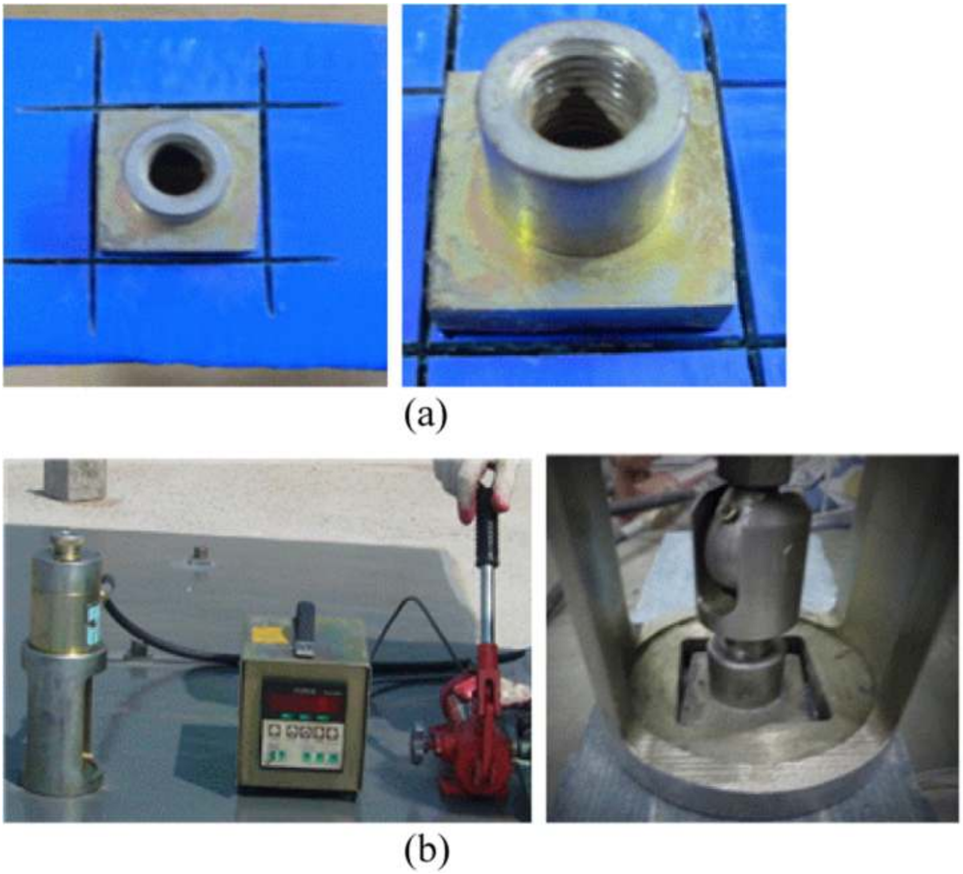

Fig. 5. (a) Dolly for pull-off test; (b) pull-off test setup.

conduction, stress transfer, failure behavior, etc. Shore hardness property tests were conducted in accordance with KS M ISO 7619–1 [24]. Hardness tester types A and D were used for the tests. The most significant difference between the type A and D testers lies in the push-pin used to measure the hardness, as shown in Fig. 6(a). The push-pin of the type D tester is sharper than that of the type A tester. Thus, hardness values greater than and less than 90° were measured using the A- and D-type durometers, respectively, as shown in Fig. 6(a). The tests were conducted using the measurement kit and specimen type shown in Fig. 6(b). Fig. 6(c) shows a photo of the test setup [24], and Fig. 7 shows the Shore hardness results. The Shore hardness test results were in the order of Case 3, 2, and 1, from high to low, with a trend of a higher NCO (%) mix ratio resulting in higher Shore hardness, similar to the tensile strength trend based on the amount of isocyanate in the prepolymer. The mechanical property test results from the STPU development study showed that Case 3 with NCO 18 % was the best mix proportion, which was used for its durability property evaluations.

4. STPU Durability Tests

PU is a material with relatively good durability in aggressive chemical environments (i.e., those containing acid, alkali, chloride, etc.). PU must satisfy the durability requirements specified in KS F 4922 [23], which include basic durability capacity limits for materials to be used in actual construction sites. However, because the main agents and hardener of the prepolymer in the STPU developed in the present study were improved and mixed independently, their durability must be demonstrated to satisfy the KS F 4922 requirements before they can be used in actual construction sites [23]. Normally, the conditions that PUs face include exposure to

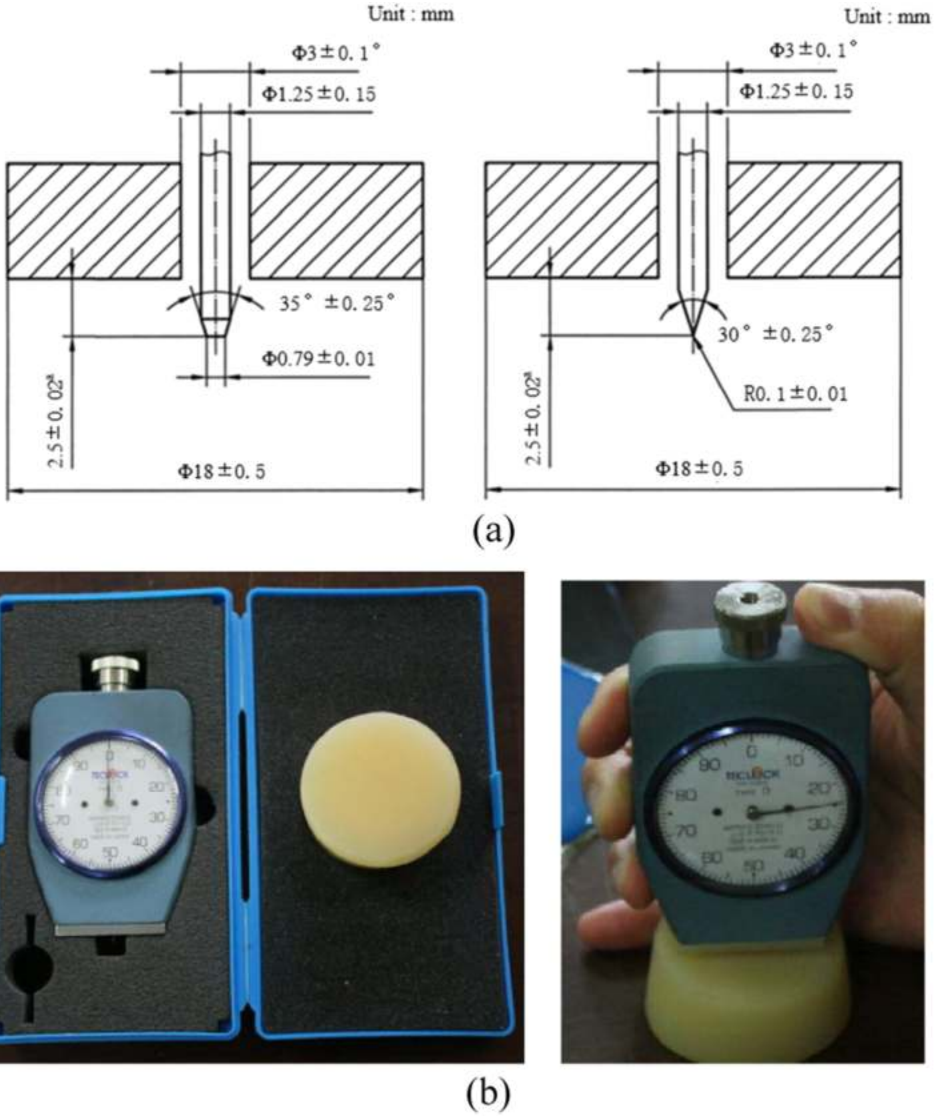

Fig. 6. (a) Type A (left) and D (right) hardness test push-pins; (b) Shore hardness test kit.

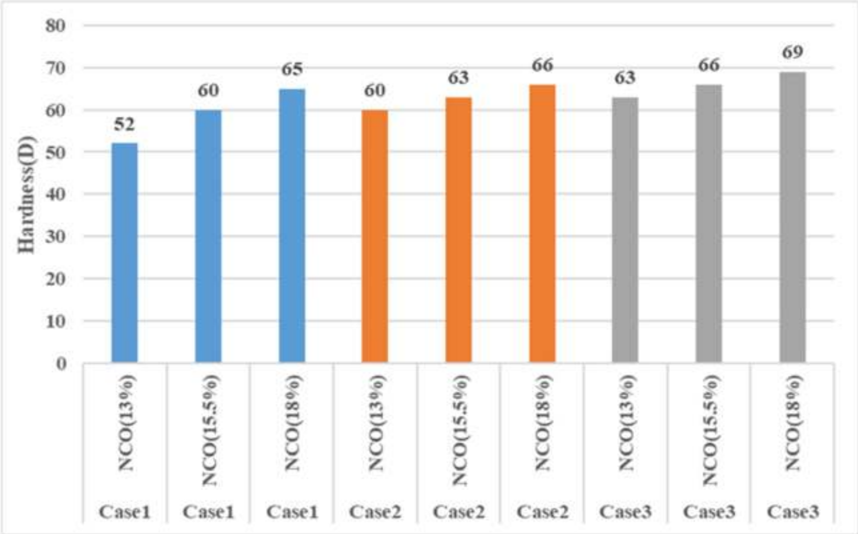

Fig. 7. Shore hardness test results.

acid rain, UV sunlight, and pollution, including pollutants in air and the alkali conditions and chloride in wind.

The STPU in this study was developed to be used to retrofit existing reinforced concrete (RC) columns or piers of bridges that are currently in service. Because RC columns are usually constantly exposed to outdoor conditions and the environment, aging deterioration occurs over time. Therefore, the aging effect of PU must be precisely understood for this material to be used as a seismic retrofitting and strengthening material for concrete structures. To determine the durability of PU against various chemical degradation factors that occur naturally or artificially, we selected acidic environments and UV exposure as weathering conditions. The freeze–thaw and carbonation exposure resistance of PU when applied to concrete specimens were also evaluated. Therefore, we tested durability under both natural service aging and chemical attack.

4.1. Acid environmental exposure test description and discussion of results

Acid environmental exposure tests were conducted in accordance with KS F 4922 [23]. The type of acid used in the test was a 2 % special-grade sulfuric acid solution specified in KS M ISO 6353–2 (R37), under an acid treatment temperature of 20 ± 2 ℃ [25]. As shown in Fig. 8, three specimens were immersed in 400 mL of the 2 % solution of sulfuric acid for 168 h (1 week). The specimens used in the tests were prepared as type 3 dumbbell specimens, as specified in KS M 6518 and described previously [22]. To evaluate the

Fig. 8. Acid environmental exposure test under acid concentration of H_2SO_4 2 % 400 mL.

durability of the STPU developed in this study, tensile strength and percent elongation were measured before and after specimens were exposed to the acidic environment, as described previously.

The results of the tensile strength and percent elongation of STPU before and after exposure to an acidic environment are presented in Table 3. For tensile strength, STPU specimens immersed in the 2 % sulfuric acid solution showed a degradation in strength of 17 %. For percent elongation, STPU specimens immersed in the 2 % sulfuric acid solution showed a degradation in percent elongation of 1 %. "The Quality Standard after Acid Treatment on Waterproof Material" specified in KS F 4922 requires the tensile strength rate before and after acid emersion to be 80–150 % and the percent elongation before and after acid immersion to be greater than 250 % [23]. The tensile strength test results after the specimens were exposed to acidic environments satisfied the requirement for 2 % (pH 0.33) sulfuric acid immersion. The percent elongation test results did not satisfy the "250 % or higher" requirement of the Korean standard. The tested STPU showed a percent elongation of 248 %, 2 % below the requirement. However, the tensile strength degradation of the specimens was only 17 %, which was relatively low. Considering the inevitable error that can occur from physical testing, the acid exposure durability performance was satisfactory.

4.2. UV sunlight exposure test description and discussion of results

UV light exposure tests were conducted in accordance with KS F 2274 [26]. A xenon-arc source, which emits more intense UV light than a UV fluorescent lamp, was used in the test. Fig. 9(a) and (b) show a photo of the xenon-arc test chamber exterior and interior, respectively. As shown in Fig. 9(b), three type 3 dumbbell STPU specimens were exposed to UV light for 1000 and 2000 h. For comparison purposes, the tensile strength and percent elongation tests were conducted on STPU specimens without and with UV light exposure. Both the tensile strength and percent elongation tests were conducted with three specimens, and the results were averaged to obtain a mean value.

The results of the tensile strength and percent elongation tests of STPU before and after exposure to UV light are presented in Table 4. With respect to tensile strength, the STPU specimens exposed to UV light for 1000 and 2000 h showed strength degradations of 39 % and 36 %, respectively. With respect to percent elongation, the STPU specimens exposed to UV light for 1000 and 2000 h showed degradations of 30 % and 41 %, respectively. "The Quality Standard after Acid Treatment on Waterproof Material" in KS F 4922 [23] requires a tensile strength greater than 16 MPa, a tensile strength rate of 50–80 %, and a percent elongation rate greater than 250 %. The tensile strength test results from UV light exposure for 2000 h satisfied the 18-MPa requirement. However, for the tensile strength and percent elongation rates, the results did not satisfy the requirements specified in the Korean standard [23]. When the UV exposure dose of 550 W/m2 was emitted in one cycle, a total of 1980 MJ/m2 and 3960 MJ/m2 UV exposure doses were emitted during 1000 and 2000 h of exposure, respectively. The total amount of UV light exposure from weather in Korea each year is approximately 270 MJ/m2. When UV light exposure values for 1000 and 2000 h are converted to exposure durations based on UV light exposure data in Korea, they are found to be equivalent to approximately 87 months and 174 months of environmental exposure time, respectively [27]. Since the percentage elongation target for the development of STPU was 250 %, the percent elongation Korean standard requirement of 250 % or better for the material applied with the UV exposure time is not logical for STPU. Therefore, the percent elongation of STPU must be lower than 250 % in this evaluation. The durations of the UV exposure test in this study were 1000 and 2000 h, which are 4 and 8 times greater than the 250-h time duration requirement of the Korean standard. The result from the tensile strength test was 18 MPa after 2000 h of UV exposure, which exceeds the requirement of 16 MPa. Therefore, the durability performance after UV exposure can be considered satisfactory. In the harsh environmental condition tests, 3 specimens are tested for acid and UV exposure test. Even though the number of the specimens is limited, the result trends from the tests are relatively distinct. However, further tests with more specimens are needed to conclusively determine the performance of STPU under harsh environmental condition.

4.3. STPU-covered concrete carbonation exposure test description and discussion of results

Carbonation exposure tests were conducted in accordance with KS F 2584 [28]. A carbonation exposure chamber was set up with environmental conditions of 20 ℃, 60 % relative humidity, and 5 % carbon dioxide (Fig. 10(a)). As shown in Fig. 10(b), the STPU developed in this study was spread onto the side surfaces of six 100 mm × 200 mm cylindrical normal-strength concrete specimens and six 100 mm × 200 mm cylindrical high-strength concrete specimens, which were placed in the chamber for 4 weeks. For the depth measurement, a phenolphthalein solution was sprayed; its color changed to violet-red where carbonation occurred. Each specimen was then sliced into two half-cylinders along the longitudinal direction. Then, 10 points at intervals of 20 mm along the height of each half-cylinder were selected for measurement of the carbonation dispersion depth. Therefore, the carbonation dispersion depth was measured from a total of 60 points in the test. Finally, the average carbonation dispersion depth was calculated and used as the carbonation depth value. The carbonation rate modulus was estimated from the results of the carbonation depth measurements and

Table 3
Acid environmental exposure test results.

	STPU	H2SO4 2 %	Ratio
Tensile Strength [MPa]	28	23	1.0: 0.83
Percent Elongation [%]	250	248	1.0: 0.99

(a) (b)

Fig. 9. UV light exposure test machine; (a) inside of chamber; (b) accelerated artificial exposure chamber.

Table 4
UV light exposure test results.

	STPU	1000 h	2000 h	Ratio
Tensile Strength [MPa]	28	17	18	1.0: 0.61: 0.64
Percent Elongation [%]	250	175	172	1.0: 0.70: 0.69

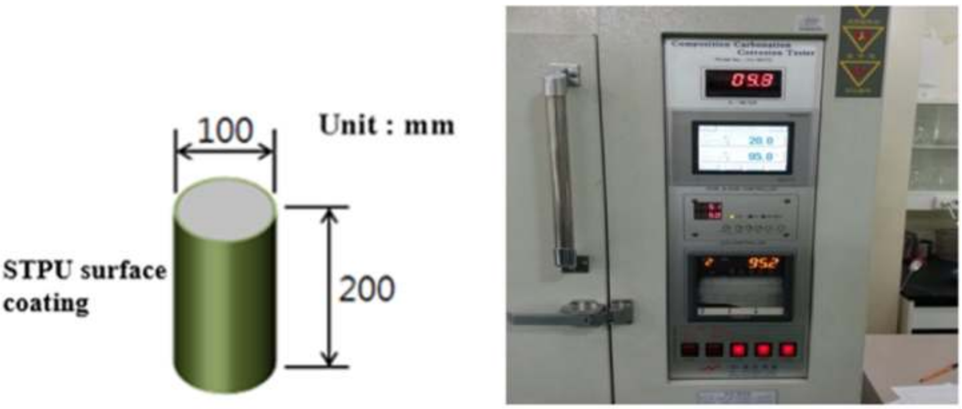

(a) (b)

Fig. 10. Concrete carbonation exposure test; (a) cylinder specimen; (b) carbonation chamber.

was calculated using Eq. 4.

$$a = d/\sqrt{t} \tag{4}$$

where a is the carbonation rate modulus, *d* is the carbonation depth (mm), and *t* is the carbonation exposure time (weeks).

The carbonation depth and carbonation rate modulus before and after carbonation exposure are shown in Table 5. STPU-applied specimens exposed to carbonation had no carbonation dispersion irrespective of the concrete strength. The carbonation exposure test results from the concrete specimens without the STPU coating and exposed for 4 weeks exhibited a carbonation depth and carbonation rate modulus of 5.87 mm and 5.5 mm, respectively. The results showed that the STPU-coated concrete specimens exhibited 27.3 % less carbonation dispersion than the uncoated concrete specimens, revealing that STPU provides good carbonation protection for concrete. Fig. 11 shows photos of the specimens sprayed with the phenolphthalein solution for the measurement of the carbonation dispersion depth.

4.4. STPU-covered concrete freeze–thaw test description and discussion of results

Freeze–thaw tests were conducted in accordance with KS F 2456 [29]. A freeze–thaw chamber was used to apply the concrete specimen center temperature of −18 ℃ during freezing and + 4 ℃ during thawing. The STPU developed in this study was sprayed onto 100 mm × 200 mm cylindrical normal- and high-strength concrete specimens. To evaluate the freeze–thaw performance of the STPU developed in this study, relative dynamic elastic modulus and compressive strength tests were conducted on the STPU-coated concrete specimens before and after 300 cycles of freezing and thawing.

As shown in Fig. 12(a), 300 cycles were applied to the specimen with one freeze–thaw cycle applied in 2–4 h inside an atmospheric chamber. The dynamic elastic modulus was measured using the measuring tool shown in Fig. 12(b) from three specimens to obtain a mean value. The mean value was used to calculate the relative dynamic elastic modulus and the durability factor using Eqs. 5 and 6, respectively.

$$P_c = \left(n_c^2/n_0^2\right) \times 100 \tag{5}$$

where P_c is the relative dynamic elastic modulus (%) after c cycles of freezing and thawing, n_o is the first resonance frequency (Hz) of the deformation vibration at 0 cycles of freezing and thawing, and n_c is first resonance frequency (Hz) of the deformation vibration at c cycles of freezing and thawing.

$$DF = (P \times N)/M \tag{6}$$

where *DF* is the durability factor of a test specimen, *P* is the relative dynamic elastic modulus at *N* cycles, *N* is the number of cycles at which the relative dynamic elastic modulus is 60 % or the number of cycles at which the exposure to freeze–thaw is terminated, and *M* is the number of cycles at which the exposure to freeze–thaw is terminated.

The results of the relative dynamic elastic modulus and compression strength tests of STPU-coated specimens before and after 300 freeze–thaw cycles are presented in Table 6. The durability factors according to the relative dynamic elastic modulus before and after 300 cycles were 74.55 % and 90.88 % without and with the STPU coating, respectively; by contrast, the compression strength degradation rates were 11.94 % and 0.97 % without and with the STPU coating, respectively. If a durability factor exceeds 95 %, then the durability is considered excellent. STPU provided good freeze–thaw protection for the concrete samples. However, because the test values are within the error margin, additional tests may be needed to further verify the freeze–thaw protection ability of STPU [30]. Because all the STPU-coated concrete specimens had slightly higher durability factors and exhibited less strength degradation than the uncoated specimens, the results indicate that the freeze–thaw durability performance can be improved by the STPU coating.

5. STPU selection for application purpose

5.1. Retrofitting application for uniaxial compression strength test description

RC cylindrical and rectangular specimens sprayed with STPU of the Case 3 (NCO18 %) mix proportion were tested under uniaxial compression loading to check the STPU's retrofitting and strengthening performance. As shown in Fig. 13, the cross-sectional dimensions were ⌀200 mm for circular specimens and 200 × 200 mm^2 for square columns with a height of 700 mm. All specimens contained 4-D16 rebars in the longitudinal direction and 4-D12 hoop rebars placed 40, 240, 460, and 660 mm from the bottom surface of the specimen. A total of 12 specimens were prepared: three STPU-sprayed circular, three bare circular, three STPU-sprayed square,

Table 5
Concrete carbonation exposure test results.

Type	Time [weeks]	Carbonation depth [mm]	Carbonation rate modulus
Uncoated	4	16.5	8.25
Side-coated (STPU-coated)	4	11.0	5.5

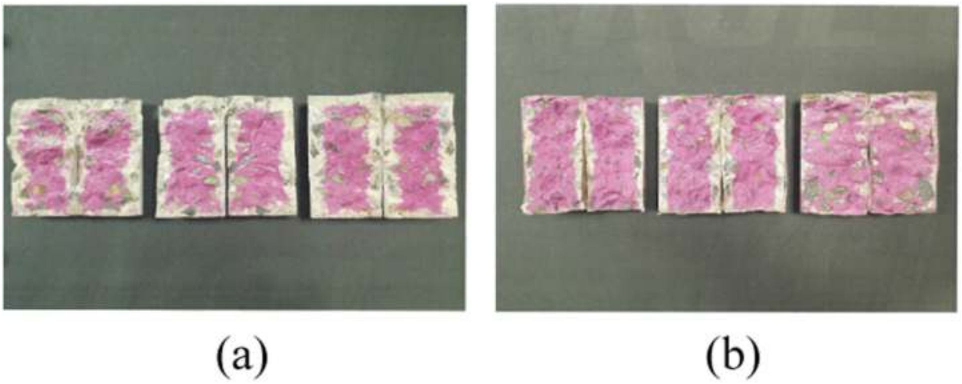

Fig. 11. Normal-strength concrete carbonation exposure test results (a) uncoated (4 weeks); (b) side-coated (4 weeks).

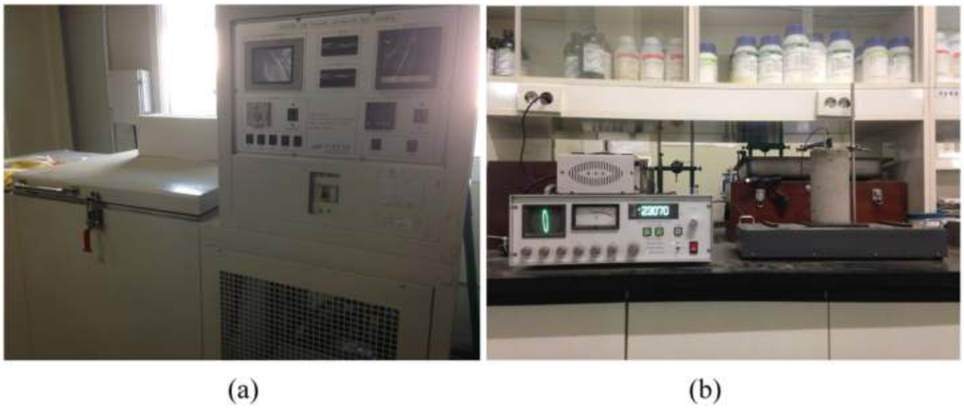

Fig. 12. (a) Freeze–thaw test machine; (b) dynamic elastic modulus measuring equipment.

Table 6
Freeze–thaw test results.

Type	Cycle	Dynamic elastic modulus [Hz]	Relative dynamic elastic modulus [%]	Compressive strength [MPa]	Reduced strength [%]
Uncoated	0	23,140	74.55	39.59	11.94
	300	19,979		34.30	
Coated	0	21,977	90.88	40.11	0.97
	300	20,951		37.64	

and three bare square RC specimens. The 5-mm thick STPU was sprayed onto the side of the specimens. Table 7 presents an outline of the specimens, and Fig. 14 shows a photo of the specimens. For compression loading, 3000 kN UTM was used with a loading rate of 0.833 mm/s.

5.2. Uniaxial compression strength test discussion of results

The experiment results of the uniaxial compression tests are presented in Table 8. The maximum load ratios between the STPU-strengthened and bare RC specimens with circular and square cross-sections were 1.14 and 1.20, respectively. Fig. 15 shows the load–displacement curves obtained from the uniaxial compression tests. The ductility of the test specimens was calculated using Eq. 7.

$$\mu = \left(\mu_f - u_{el}\right)/u_{el} \tag{7}$$

where μ is the ductility of the test specimen, u_f is the displacement when the specimen failure occurs, and u_{el} is the displacement until the specimen undergoes elastic behavior.

The ductility values of the bare and STPU-strengthened square specimens were 3.20 and 6.22, respectively, while those of the bare and STPU-strengthened circular specimens were 0.52 and 2.91, respectively. Maximum load P_{max} of C-STPU had higher values than S-

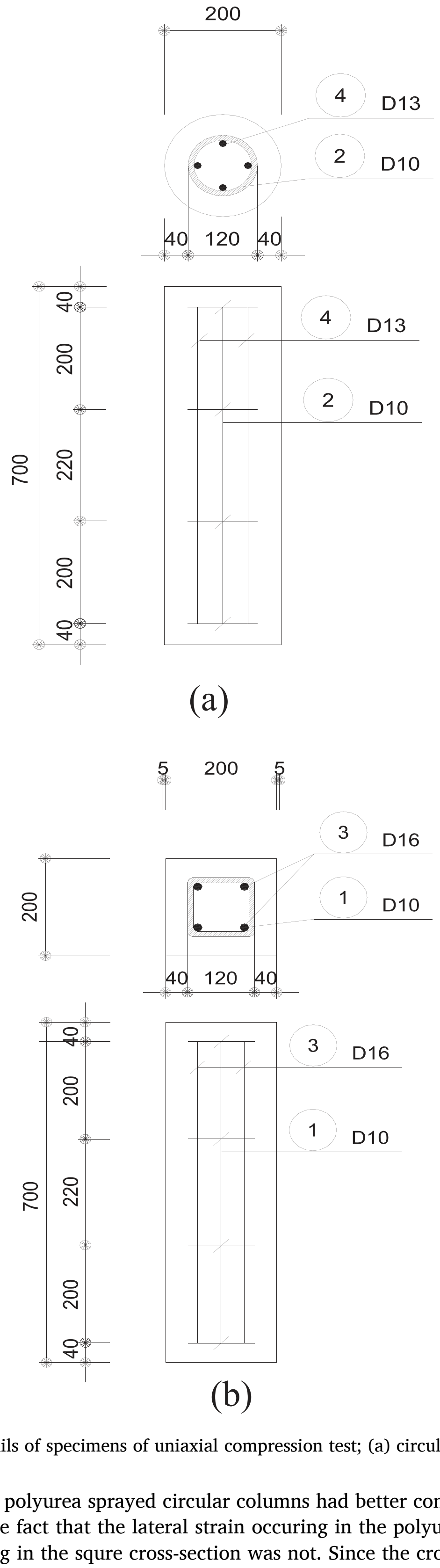

Fig. 13. Details of specimens of uniaxial compression test; (a) circular; (b) square.

STPU, which indirectly indicate that the polyurea sprayed circular columns had better confinement effect than square column. The better confinement effect comes from the fact that the lateral strain occuring in the polyurea was continuous in the circular cross-section whereas the later strain occurring in the squre cross-section was not. Since the cross-sectional area of S-STPU was 121.5 % of C-STPU, the ductility improvement in S-STPU was approximately two folds to that in C-STPU. Unlike the bare RC specimens, STPU-

Table 7
Outline of uniaxial compression test specimens.

Specimen	Type	Retrofitting material	Specimens [ea]
C-RC	Circular	Non-STPU	3
C-STPU	Circular	STPU 5 mm	3
S-RC	Square	Non-STPU	3
S-STPU	Square	STPU 5 mm	3
Total			12

Fig. 14. Photo of uniaxial compression test RC specimens with (white) and without STPU strengthening (gray).

Table 8
Uniaxial compression test results.

Specimen	P_{Max} [kN]	Avg. P_{Max} [kN]	Avg. P_{Max} ratio	Ductility [m/mm]
C-RC-01	996.3	973.70	1.00	0.52
C-RC-02	947.3			
C-RC-03	977.5			
C-STPU-01	1062.3	1112.30	1.14	2.91
C-STPU-02	1117.8			
C-STPU-03	1156.8			
S-RC-01	904.8	867.80	1.00	3.20
S-RC-02	823.7			
S-RC-03	874.9			
S-STPU-01	1074.1	1038.77	1.20	6.22
S-STPU-02	990.4			
S-STPU-03	1051.8			

strengthened specimens showed much longer displacement behavior until a sudden drop in the load. This type of ductile behavior is attributable to the STPU layer applying confinement pressure on the concrete specimen, thereby delaying crack formation. Fig. 16 shows photos of the failure behavior of the circular and square cross-sectional specimens. As shown in the photos, to eliminate premature failure at the ends of the specimens, steel caps were attached to the specimens before loading. Fig. 16 shows that the STPU-strengthened circular and square specimens showed a wrinkled STPU layer, indicating that STPU resisted the bulging behavior of the concrete specimen from the confinement effect. However, in the bare specimens, macro-crack splitting occurred at the center of the specimens in the longitudinal direction, which led to the ultimate failure of the specimens. STPU applied on RC column by spraying without any other strengthening material such as CFRP or GFRP sheets can improve the static load bearing capacity of the member. However, when STPU is applied with CFRP or GFRP sheets as a hybrid strengthening material, cyclic loading and blast or impact resistance capacities of the strengthened RC member can be improved significantly.

With respect to carbon footprint of the newly developed STPU, there is no advantage in using STPU as a retrofitting material compared to using CFRP or GFRP sheet. However, when STPU strengthening is compared to the member replacement of damaged RC columns, a construction of a new square RC column with dimensions of 400 × 400 × 3000 mm would induce carbon emission of 1000 kg [31] whereas STPU spraying would induce no carbon emission, which is a significant reduction in carbon emission amount.

One important technical study that needs to be further undertaken is the evaluation of interface characteristic between STPU and concrete surface. There have been many study results published on the interface bond performance of FRP sheet and concrete surface in the past. However, there is no available study result on the interface bond performance evaluation between Polyurea and concrete surface. Therefore, by using various non-destructive testing (NDT) methods, the interface bond performance of STPU must be studied

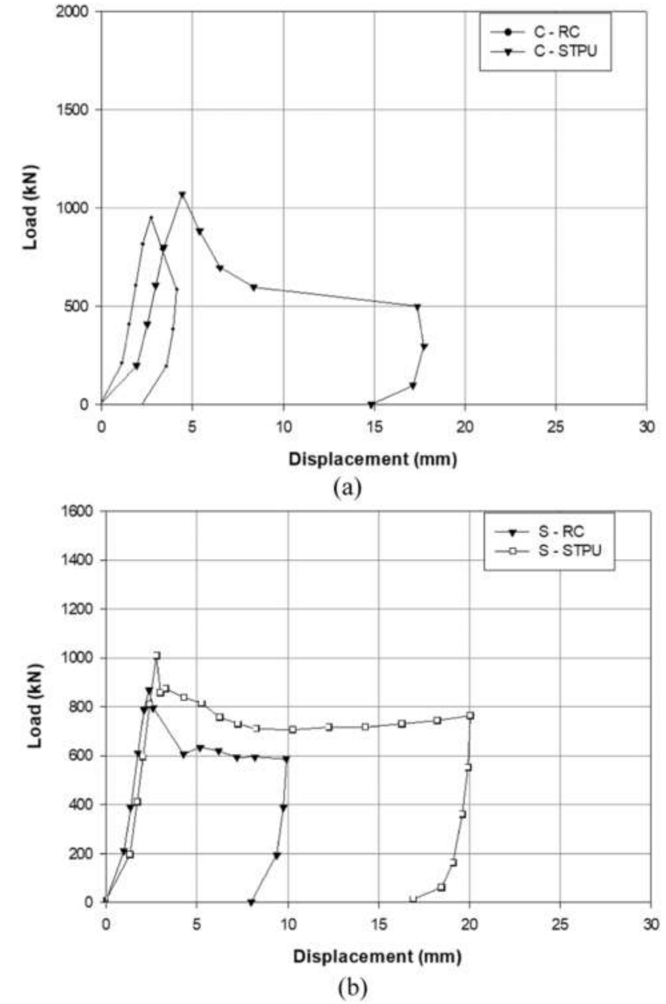

Fig. 15. Load–displacement curves of uniaxial compression tests; (a) circular specimen; (b) square specimen.

in the future to insure reliability of retrofitting of RC structures by STPU surface spraying [32,33].

6. Conclusions

The mechanical and durability properties of STPU were evaluated through tensile strength, percent elongation, pull-off, Shore hardness, acid environmental exposure, UV sunlight exposure, STPU-covered concrete carbonation exposure, and STPU-covered concrete freeze–thaw tests. Uniaxial compression tests were conducted on circular and square RC specimens strengthened with STPU manufactured using an optimal mix proportion deduced from the results of this study. The test results are summarized as follows.

1) To develop STPU, a high tensile strength and low percent elongation are needed. The results of the mechanical property tests showed that the tensile strength increased with the amount of isocyanate and that the percent elongation decreased as the NCO mix ratio increased in all cases. The mechanical property test results showed that Case 3 with NCO 18 % was the best mix proportion for STPU.
2) From an acid environmental test, the STPU specimens immersed in a 2 % sulfuric acid solution showed degradation in tensile strength of approximately 17 %. From UV sunlight exposure tests, STPU specimens exposed to a xenon-arc source for 1000 h and 2000 h showed degradations in tensile strength of 39 % and 36 %, respectively. The tensile strength results for STPU exposed to acidic and UV light environments satisfied the Korean standard requirements, indicating that STPU shows excellent durability.
3) From concrete carbonation exposure tests, the STPU-coated concrete specimens exhibited 33.34 % less carbonation exposure than uncoated concrete specimens, revealing that STPU is an excellent carbonation protection material for concrete.
4) From STPU-covered concrete freeze–thaw tests, the specimens with all sides coated with STPU exhibited a slightly higher durability factor and a lower level of degradation in strength than the uncovered specimens, indicating slightly better freeze–thaw resistance when STPU is used.

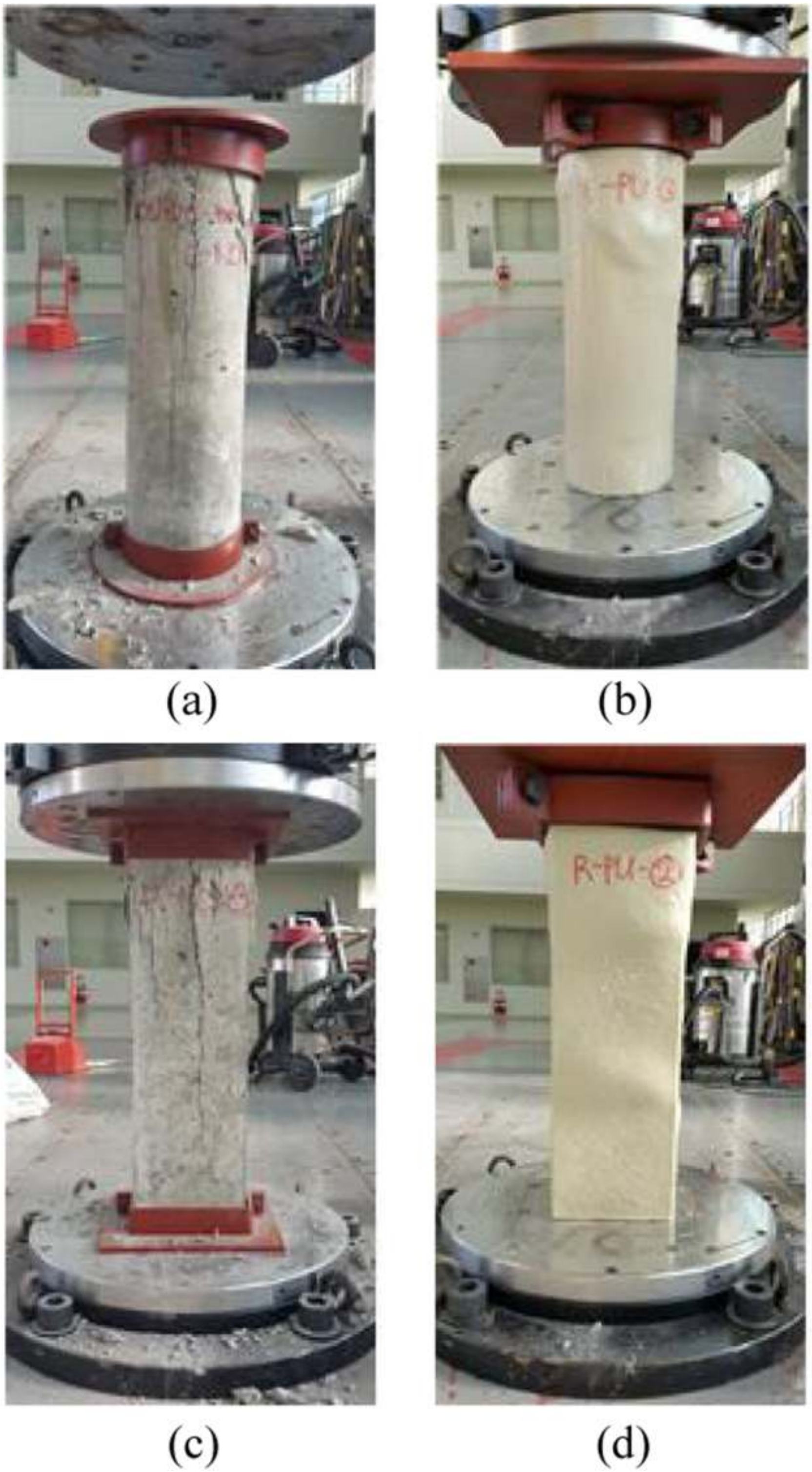

Fig. 16. Failure behavior of uniaxial compression tested specimens; (a) C-RC; (b) C-STPU; (c) S-RC; (d) S-STPU.

5) From uniaxial compression strength tests, the maximum load for the circular and square specimens with STPU strengthening increased by 114 % and 120 % compared with the bare RC specimens, respectively. Circular and square STPU-strengthened specimens exhibited much greater ductility than the bare specimens because of the confinement and crack-delaying effect induced by STPU strengthening.

Declaration of Competing Interest

The authors declare that they have no known competing financial interests or personal relationships that could have appeared to influence the work reported in this paper.

Data availability

Data will be made available on request.

Acknowledgements

This work was supported by the Korea Institute of Energy Technology Evaluation and Planning (KETEP) granted financial resource from the Ministry of Trade, Industry & Energy, Republic of Korea (No.20202020800060). Also, this research was supported by Korea Agency for Infrastructure Technology Advancement(KAIA) grant funded by the Ministry of Land, Infrastructure and Transport (Grant 21NANO-B158359-02).

References

[1] Korea Meteorological Administration (KMA), Earthquake, Korea. https://www.weather.go.kr/plus/eqkvol/domesticlist.jsp?startTm=2016–01-01&endTm=2016–1230&startSize=5.0&endSize=5.5&startLat=&endLat=&startLon=&endLon=&lat=&lon=&dist=&keyword=&schOption=T&x=37&y=7, September, 2016.
[2] Nam H.W. The Status of Earthquake Occurrence in Korea in 2013. Press Release of Korea Meteorological Administration, Korea, 2014.
[3] J.F. Bonacci, M. Maalej, Behavioral trends of RC beams strengthened with externally bonded FRP, J. Compos. Constr. 5 (2) (2001) 102–113.
[4] M. Zubair, N.D. Mu'azu, M. Nasir, et al., Cellulose nanocrystals from office paper waste for green mortar: process optimization modeling, characterization, and mechanical properties, Arab J. Sci. Eng. 47 (2022) 5377–5393, https://doi.org/10.1007/s13369-022-06609-8.
[5] M.A. Aziz, M. Zubair, M. Saleem, Development and testing of cellulose nanocrystal-based concrete, Case Stud. Constr. Mater. 15 (2021), e00761, https://doi.org/10.1016/j.cscm.2021.e00761.
[6] X.Z. Lu, J.G. Teng, L.P. Ye, et al., Bond–slip models for FRP Sheets/plates bonded to concrete, Eng. Struct. 27 (6) (2005) 920–937.
[7] J.W. Nam, H.J. Kim, S.B. Kim, et al., Numerical evaluation of the retrofit effectiveness for GFRP retrofitted concrete slab subjected to blast pressure, Compos. Struct. 92 (5) (2010) 1212–1222.
[8] Z.F. Chen, L.L. Wan, S. Lee, et al., Evaluation of CFRP, GFRP and BFRP material systems for the strengthening of RC slabs, J. Reinf. Plast. Compos. 27 (12) (2008) 1233–1243.
[9] M. Kwon, P.B. Shing, C. Mallare, et al., Seismic resistance of RC bent caps in elevated mass transit structures, Earthq. Spectra 27 (1) (2011) 67–88.
[10] H.L. Cheng, E.D. Sotelino, W.F. Chen, Strength estimation for FRP wrapped reinforced concrete columns, Steel Compos. Struct. 2 (1) (2002) 1–20.
[11] M.N.S. Hadi, Behaviour of FRP wrapped normal strength concrete columns under eccentric loading, Compos. Struct. 72 (4) (2006) 503–511.
[12] M. Maalej, S. Tanwongsval, P. Paramasivam, Modelling of rectangular RC columns strengthened with FRP, Cem. Concr. Compos. 25 (2) (2003) 263–276.
[13] M.H. Harajli, Z. Khalil, F.R.P. Seismic, Retrofit of bond-critical regions in circular RC columns: validation of proposed design methods, Acids Struct. J. 105 (6) (2008) 760.
[14] H. Lee, H. Jang, W. Chung, Effect of recycled concrete on the flexural behavior of concrete-filled FRP tubes, Int. J. Concr. Struct. Mater. 13 (1) (2019) 53–62.
[15] M. Ju, S. Lee, C. Park, Response of Glass Fiber Reinforced Polymer (GFRP)-steel hybrid reinforcing bar in uniaxial tension, Int. J. Concr. Struct. Mater. 11 (4) (2017) 677–686.
[16] S.Y. Ghanem, I.E. Harik, Concentrically loaded circular RC columns partially confined with FRP, Int. J. Concr. Struct. Mater. 12 (1) (2018) 597–613.
[17] S.B. Kim, J.H.J. Kim, H.S. Choi, et al., Development and applicability evaluation of high performance poly-urea for RC construction reinforcement, J. Korean Soc. Civ. Eng. 30 (2) (2010) 169–176 (In Korea).
[18] J.C. Park, S.W. Lee, S.B. Lim, et al., Performance evaluation of RC slab strengthened by stiff type polyurea, J. Korean Soc. Civ. Eng. 31 (6) (2011) 457–464 (In Korea).
[19] J.H.J. Kim, J.C. Park, S.W. Lee, et al., Evaluation of strengthening performance of stiff type polyurea retrofitted RC slab based on attachment procedure, J. Korea Concr. Inst. 23 (4) (2011) 511–520 (In Korea).
[20] Kim J.H.J., Yi N.H., Kim S.B., et al. Experiment study on blast loading response of FRP-retrofitted RC slab structures. In: The Second official International Conference of International Institute for FRP in Construction for Asia-Pacific Region, Seoul, Korea, 9 December -11 December 2009, 3(4): 533–538.
[21] N.M.K. Lamba, K.A. Woodhouse, S.L. Cooper. Polyurethanes in Biomedical Applications, 1st ed..,, CRC Press, United States of America, 1998, pp. 14–23.
[22] KS M 6518, Physical Test Methods for Vulcanized Rubber, Korea Standards Association, Korea (2006).
[23] KS F 4922: 2007. Polyurea Resin Waterproofing Membrane Coating. Korea Standards Association, Korea.
[24] KS M ISO 7619–1: 2011. Rubber, Vulcanized or Thermoplastic-Determination of Indentation Hardness-Part 1: Durometer method (Shore hardness). Korea Standards Association, Korea.
[25] KS M ISO 6353–2 (R37): 2012. Reagents for chemical analysis – Part 2: Specifications – First Series [Sulfuric acid]. Korea Standards Association, Korea.
[26] KS F 2274: 2002. Recommended Practice for Accelerated Artificial Exposure of Plastics Building Materials. Korea Standards Association, Korea.
[27] Kim Y.S., Choi M.I., Kim C.M., et al. A Study of Corona Discharge in Polymer Insulators by Artificial UV Radiation. *The Transactions of the Korean Institute of Electrical Engineers* 2013; 17(6): 21–30. (In Korea).
[28] KS F 2584: 2010. Standard Test Method for Accelerated Carbonation of Concrete. Korea Standards Association, Korea.
[29] KS F 2456: 2010. Standard Test Method for Resistance of Concrete to Rapid Freezing and Thawing. Korea Standards Association, Korea.
[30] Kim T.K. Performance Based Evaluation of Concrete for Strength and Durability Considering Curing under Extreme Conditions Produced by Climate Change. PhD thesis, Yonsei University, Korea, 2016.

[31] M. Sabău, D.V. Bompa, L.F. Silva, Comparative carbon emission assessments of recycled and natural aggregate concrete: Environmental influence of cement content, Geosci. Front. 12 (6) (2021), 101235, https://doi.org/10.1016/j.gsf.2021.101235.
[32] M. Saleem, H. Gutierrez, Using artificial neural network and non-destructive test for crack detection in concrete surrounding the embedded steel reinforcement, Struct. Concr. 22 (5) (2021) 2849–2867, https://doi.org/10.1002/suco.202000767.
[33] M. Saleem, A. Hosoda, Latin hypercube sensitivity analysis and non-destructive test to evaluate the pull-out strength of steel anchor bolts embedded in concrete, Constr. Build. Mater. 290 (2021), 123256, https://doi.org/10.1016/j.conbuildmat.2021.123256.